Fibre laser cutting: the use of carbon-filled acrylic as a qualitative and quantitative analysis tool

H. Atiyah[1], J. Powell[2], D. Petring[3], S.Stoyanov[3], K.T. Voisey[1]

1. Faculty of Engineering, The University of Nottingham, Nottingham NG7 2RD, UK.

2. Dept. of Engineering Sciences and Mathematics. Lulea University of Technology. SE-97187 Lulea, Sweden.

3. Fraunhofer Institute for Laser Technology ILT,52074 Aachen, Germany.

Abstract

The use of carbon filled black acrylic (CFBA) as a quantitative and qualitative analytical tool for fibre laser cutting is investigated. In the qualitative work CFBA targets placed below the laser cutting zone when cutting stainless steel showed a distinctive 'leaf' shaped evaporation crater which can provide information about the nature of the reflections taking place in the cut zone. Quantitative measurements have revealed a specific evaporation energy of 3.4J/mm^3 for CFBA. However, this figure is only applicable when considering intense beams when the CFBA target is stationary with respect to the laser beam.

Key Words: laser beam cutting; laser diagnostics; fibre laser; carbon filled black acrylic.

1. Introduction.

Earlier work by Powell et al. [1] divided the energy input to the cutting zone into three categories;

a. Energy used in generating a cut
b. Primary losses (i.e. reflected or transmitted energy which leaves the cutting zone as light with the same wavelength as the incident laser)
c. Secondary losses (i.e. conductive, convective and radiative thermal losses from the cutting zone)

The work included an experiment, described in figure 1a, in which transparent acrylic (poly methyl methacrylate) target blocks were used to absorb the primary (reflected and transmitted) losses from CO_2 laser cutting. The evaporation pattern created by the absorption of the laser energy provided quantitative and qualitative information about the transmission and reflection of light in the cutting zone. A typical result from this work is presented in figure 1b, showing that the transmitted and reflected light combines to form an interference pattern.

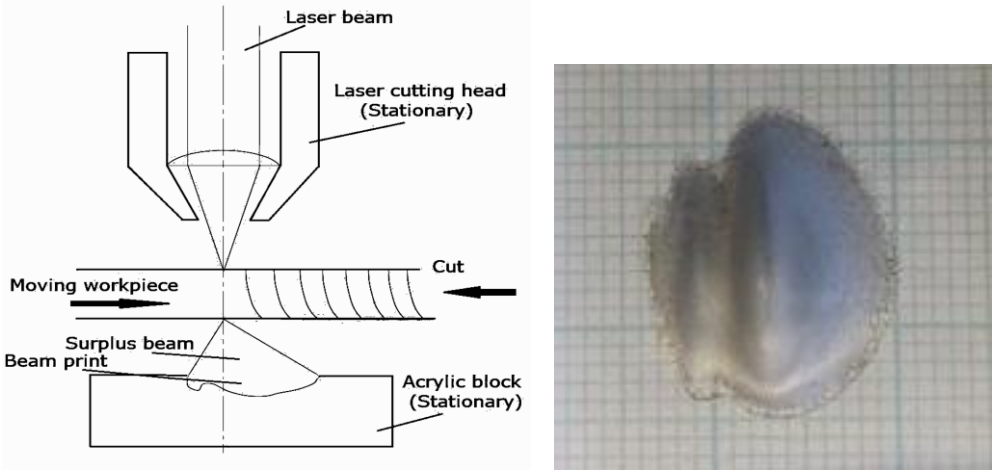

Figure 1. Collection of light escaping from the bottom of the cut zone; a. Experimental set-up. b. Beam print showing evidence of interference between the transmitted and reflected energy [1].

Clear acrylic is readily evaporated by CO_2 laser light because it is highly absorptive at a wavelength of 10.6 microns, has a low thermal conductivity and decomposes at low temperatures. It has been used since the 1970's as a cheap, convenient material for identifying laser beam quality (beam circularity and mode type) and the beam's position in the optical chain between the laser resonator and the workpiece [2]. This includes the generation of qualitative 'mode prints' [3] to check beam circularity, axial symmetry and TEM mode. In the 1980's Sarchin [4] reported on work by Keilmann which demonstrated that mode prints of this type could be relied upon as a map of the energy distribution in the beam if their depth was less than three times their width.

Work by Miyamoto et al. [5] identified the specific energy of ablation for clear acrylic evaporated by CO_2 laser as $3kJ/cm^3$. This allowed the use of acrylic for quantitative measurements of laser beam power and, via the use of energy balance equations [6], primary laser beam power losses during laser cutting [7-9].

Clear acrylic cannot be used in conjunction with fibre laser beams because the material is transparent at the fibre laser wavelength of approximately 1 µm. However, work with Nd:YAG laser beams has established that certain black grades of acrylic are highly absorbing of 1 µm wavelength light [10, 11]. (It should be noted that there are various methods of manufacturing black acrylic, and only the carbon-filled opaque grades are suitable for absorbing 1 µm wavelength light.)

In the case of CO_2 lasers and clear acrylic, the beam is directly absorbed by the polymethyl methacrylate molecules. The material has a low melting point of approximately 160 ^oC and, when the liquid is heated to approximately 300 ^oC by a CO_2 laser beam it depolymerises [12], giving off a vapour/gas of the monomer ($C_5O_2H_8$).

The evaporation of carbon-filled black acrylic by one micron wavelength light is, on the other hand, a two stage process. The laser beam passes through the polymer but is absorbed by the carbon particles held in suspension in the acrylic. The carbon particles heat up and pass on heat to the surrounding polymer molecules until they depolymerise and evaporate.

Previous attempts to use carbon-filled black acrylic to quantify primary energy losses of one micron 1 μm wavelength light have reported that the energy required to evaporate a unit volume of material increased with increasing speed [13, 14]. This was attributed to the lower interaction times limiting the effectiveness of the two stage material removal mechanism [14]. Scintilla et al. [9, 14] attempted to compensate for this speed dependency by employing second order polynomials and regression equations which involved functions dependant on laser power and cutting speed. This approach gave values for the specific ablation energy of black acrylic between 6.5 and 14.6 J/mm^3.

This paper begins by presenting the results of a series of experiments which give qualitative information about the primary losses of the cutting process (i.e. laser light which is reflected off, or transmitted through, the cutting zone). The second part of the paper determines the specific ablation energy of carbon filled black acrylic and discusses the application of this result to the quantitative measurement of primary losses from the cutting zone.

2. Experimental work.

2.1 Qualitative analysis of the primary losses from the cut zone

Using an experimental set-up similar to that shown in figure 1a (but employing carbon filled black acrylic and a horizontal air jet above the evaporation zone to disperse the evaporating smoke plume) a number of experimental runs were carried out. It is important to note that the carbon filled black acrylic and the laser beam remained stationary with respect to each other throughout this experiment. Material was fed from left to right in Fig 1a, producing a cut front

that was stationary with respect to the laser beam and hence a stationary pattern of irradiation on the surface of the black acrylic due to primary losses.

An IPG YLR-2000 fibre laser with a 1.07 μm wavelength and a maximum power of 2000 W was used for these experiments. The beam was delivered via a 200μm delivery fibre to a Precitec YK25 cutting head housing a 125 mm focal length collimating lens and a 120 mm focal length focussing lens. The beam left the cutting head via a 1 mm diameter nozzle through which nitrogen assist gas was delivered coaxially with the laser beam. The carbon filled black acrylic was manufactured by Astari.

The high absorptivity of carbon filled acrylic, combined with its high evaporation efficiency and low thermal conductivity, means that a laser-evaporated beam print will be a good first order approximation of the energy distribution of the beam exiting the bottom of the cut zone at any point (as long as the depth to width ratio of the beam print remains below 3:1). However, a number of factors must be considered when observing these beam prints;

1. There is an energy density threshold for any particular laser-material interaction. When a moving beam is involved (as it is in this case) this energy density threshold is a function of the power density and the interaction time (the interaction time is a function of the movement speed).
2. The laser beam diverges rapidly as it exits the bottom of the cut zone. This is a more important consideration for fibre lasers than it is for their CO_2 counterparts because the fibre laser beam undergoes multiple reflections inside the cutting zone and this increases the divergence angle from the cutting zone exit (see discussion around figure 15).
3. There will be an absorption/reflection/scattering effect as the beam interacts with the particles in its path which have just left the bottom of the cut zone.

4. As will be explained in the next section on quantitative measurements, it is important to ensure that the plume of smoke given off by the evaporation of carbon filled acrylic is dispersed by an air jet in order to provide a clear passage for the laser beam. If the laser beam has to pass though the plume it will be partially absorbed and scattered by the carbon particles in the smoke.

These points will be addressed in the following discussion.

The results of the beam print tests were completely different from those obtained from CO_2 laser cutting. Typical beam prints of the beam leaving the bottom of the cutting zone are presented in figure 2.

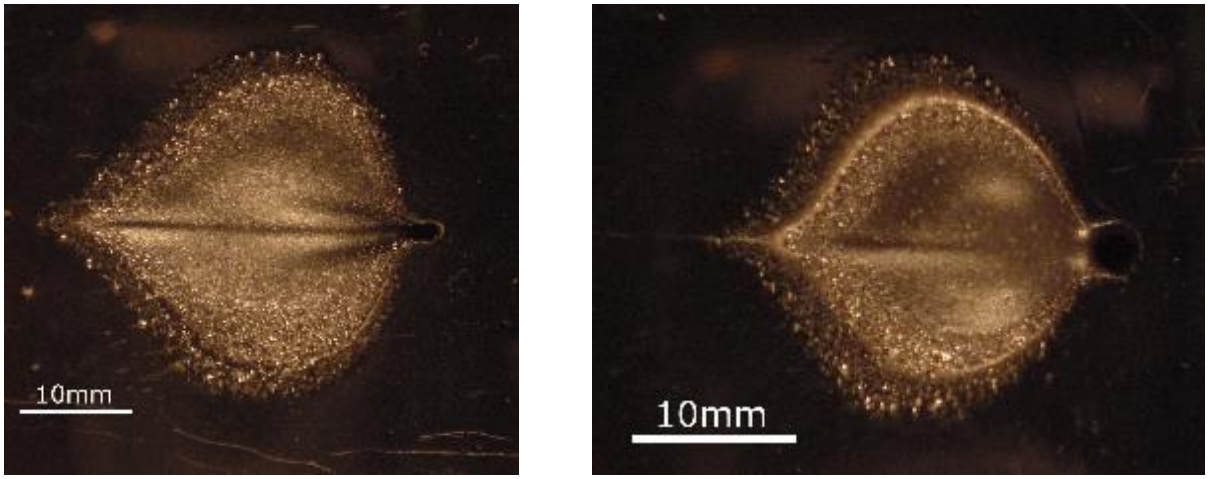

Figure 2. Typical 'leaf print' evaporation patterns taken from below the cutting zone. a. Print taken 30mm below the cutting zone when cutting 6mm stainless steel at 0.72m/min. b. Print taken 30mm below the cutting zone when cutting 3mm stainless steel at 2.57m/min. (laser power 1850W, cutting gas pressure 13 bar for 6mm and laser power 1780W, cutting gas pressure 10 bar for 3mm)

Distinctive 'Leaf print' evaporation patterns similar to those shown in figure 2 were found under almost all experimental conditions investigated during this work. Figures 2a and 2b show results from 6 and 3mm thick samples cut at 0.72m/min and 2.57m/min respectively but the

leaf prints are surprisingly similar. Figure 3 presents a 3D profile image of a typical leaf print, figure 5 shows the orientation of the leaf print with respect to the cut front.

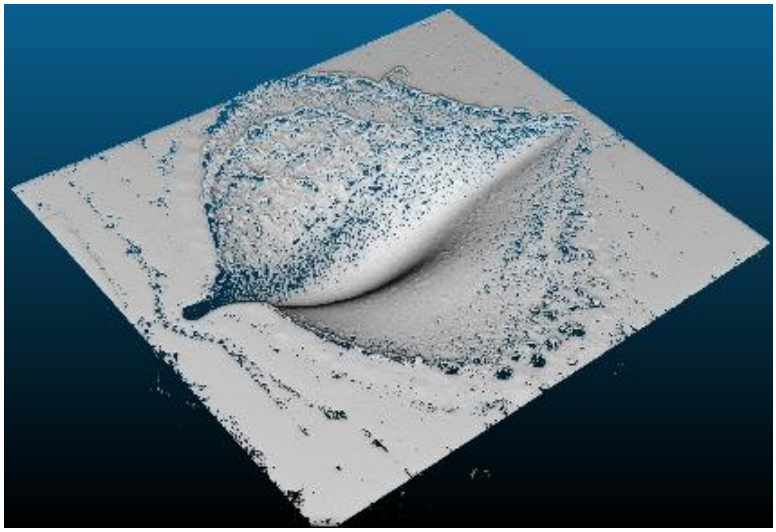

Figure 3. 3D profile of leaf print taken 23.5mm below the cutting zone when cutting 6mm thick stainless steel at 0.72m/min (laser power 1850W and cutting gas pressure 13bar)

In each case there is clear evidence of a deeper evaporated hole at the 'stem' end of the leaf, which was largely created by the vertically impinging transmitted beam. The shallower 'leaf' is an evaporation pattern created by the reflected portion of the beam. This consists of two wings joined by a central, deeper line.

Some of these features of the leaf print have been replicated by using CALCut software [15, 16] to calculate the geometry of the cutting front and Zemax software to calculate the resulting power density distribution below the cutting kerf. Figure 4 shows evidence of the high energy density spot at the stem end together with indications of a central line surrounded by widespread symmetrical energy density which fades with distance from the central line. At this stage the CALCut software does not take into account the interaction of the beam with the particles leaving the bottom of the cutting zone and this may account for the discrepancies between figure 2 and figure 4.

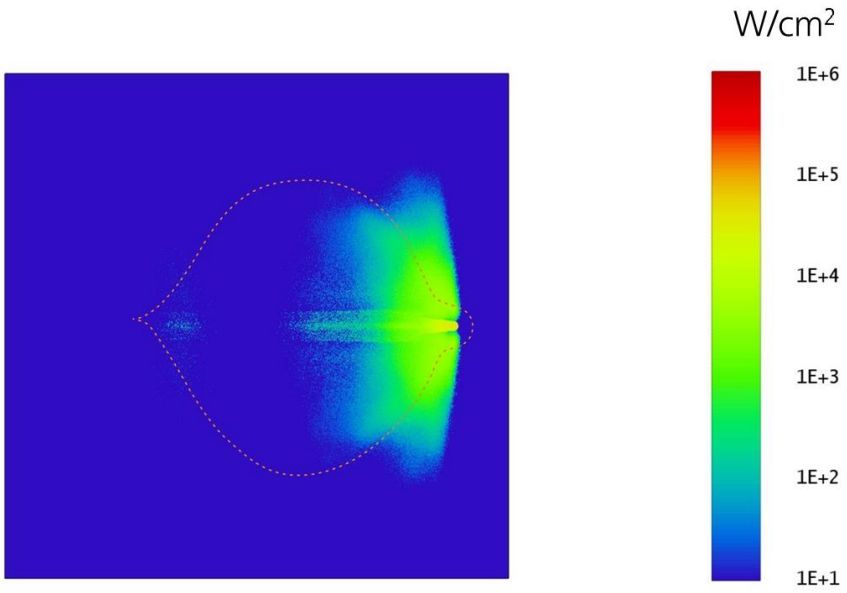

Figure 4. A theoretical calculation (using CALCut and Zemax software [15, 16]) of the primary losses emitted from the cut zone showing some of the same features as the experimental leaf traces shown in figure 2. The experimental result for the 3mm thick case is shown as a dashed line, the simulated power density distribution is presented as a logarithmic colour scale.

Figure 5 is a schematic of the creation of a leaf print below the cut zone. It seems clear that the 'stem' of the leaf is a deeper hole created by the transmitted beam whereas the body of the leaf is an evaporated pattern related to the part of the beam which has been reflected from the cutting zone and/or scattered by the stream of droplets leaving the bottom of the cutting zone. This figure has been drawn to scale and demonstrates the wide angle of divergence of the beam as it leaves the cutting zone.

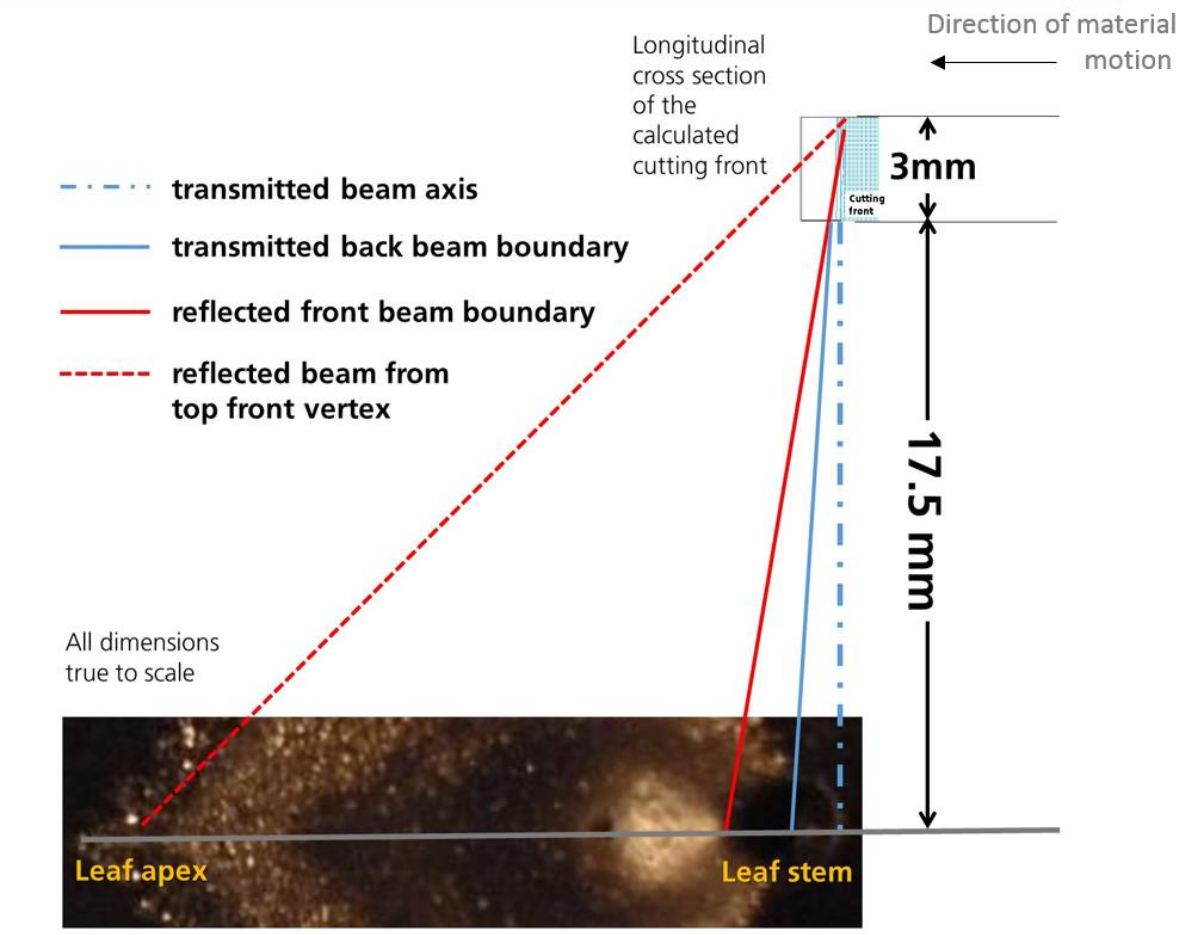

Figure 5. A schematic showing how the 'leaf' pattern is a combination of transmitted and reflected laser light.

Figure 6 presents photographs of leaf prints taken using a single set of cutting conditions at different distances from the bottom of the cutting zone. One main point of interest is that, although the detailed shape of the leaf changes slightly, the overall size of the print (large red circles) does not substantially change even though the distance from the cutting zone has approximately doubled, from 17.5mm to 35.5mm. It is clear from figure 5, and from the fact that the 'stem' hole diameter increases linearly with distance, that the reflected portion of the beam must also be growing in diameter. The lack of increase in the diameter of the body of the leaf print must therefore be associated with a threshold effect. The reflected beam gets broader with distance but the outer wings of the beam do not exceed the damage threshold and are

therefore not recorded in the print. It is clear therefore that leaf prints of this type are useful from a qualitative point of view but are unreliable as a quantitative measure of the power leaving the bottom of the cutting zone.

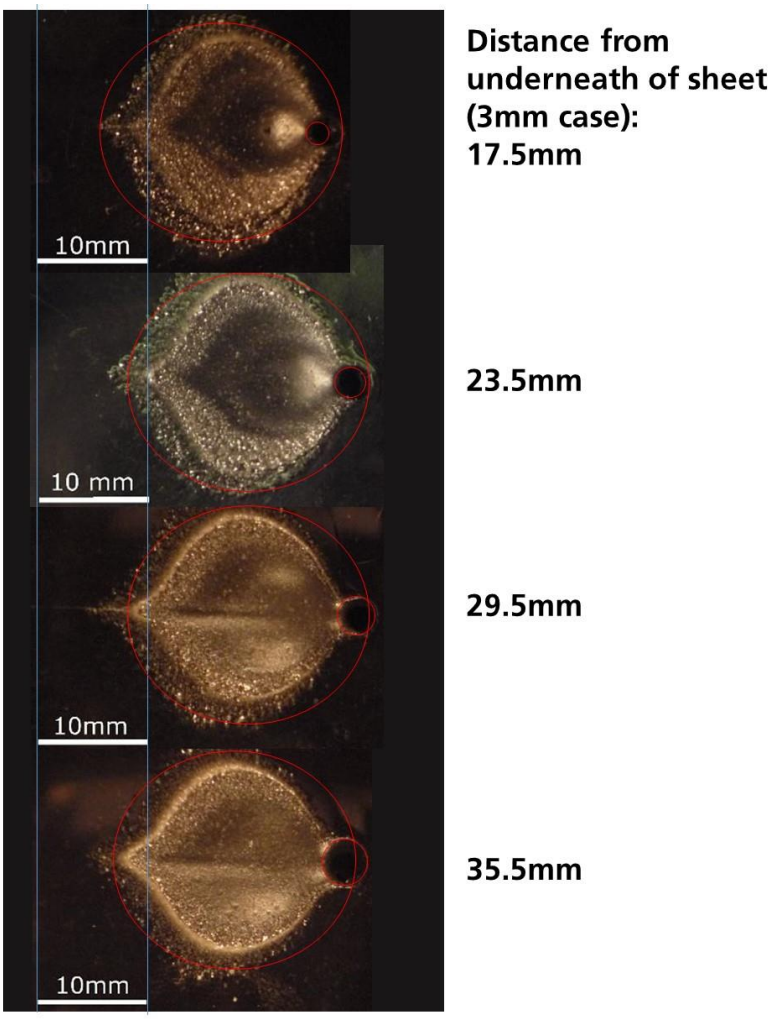

Figure 6. Leaf prints taken under the same cutting parameters at different distances from the bottom of the cutting zone.

From a quantitative point of view it is interesting that the leaf prints taken at a larger distance from the cutting zone show a more pronounced central line, which is probably the contribution of reflections from the central portion of the cutting front. In the prints taken closer to the cutting zone this deeper central line is integrated out in the generally more energetic evaporation event taking place as a result of there being a higher power density

The information presented in this section clearly shows that carbon filled black acrylic can be useful in gathering qualitative information about one micron wavelength laser beams. The situation with regards to quantitative information will now be investigated in the following section, which presents data about the specific ablation energy of the material.

2.2. Quantitative measurements of laser power; the specific ablation energy of carbon-filled black acrylic exposed to a fibre laser beam.

In order to establish the specific ablation energy of the carbon filled acrylic the laser beam was vertically incident on a stack of 3 mm thick sheets of the material (see figure 7). For the majority of this specific ablation energy work the focal plane was positioned 5 mm above the target, generating a spot diameter on the top surface of approximately 0.8 mm. Laser powers of 400 W - 1000 W were used with irradiation times ranging from 0.1 to 1.0 s, as shown in table 1.

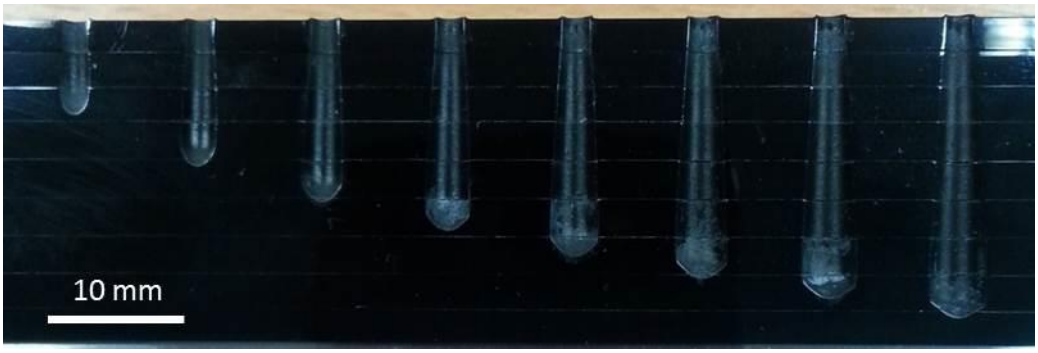

Figure 7. Holes evaporated from stacks of 3mm sheets of black acrylic.

The majority of the work was carried out with 2 bar gauge pressure nitrogen assist gas. Additional experiments were carried out with 1 bar, as well as without any assist gas, to determine the effect of assist gas flow on the evaporation process.

Power (W)	Irradiation time (s)									
400	0.1	0.2	0.3	0.4	0.5	0.6	0.7	0.8	0.9	1.0
600	0.1	0.2	0.3	0.4	0.5	0.6	0.7	0.8	0.9	1.0
800	0.1	0.2	0.3	0.4	0.5	0.6	0.7	0.8	0.9	1.0
1000	0.1	0.2	0.3	0.4	0.5	0.6	0.7	0.8	0.9	1.0

Table 1. The laser powers and irradiation times used.

Stacks of 3mm sheets were used as the target material because this allowed accurate measurement of the evaporated holes. As seen in figure 7, the holes shared a common shape, that of an expanding cone with a hemispherical bottom cap. The stack could be split open after irradiation and the hole diameter measured at 3 mm depth intervals via optical microscopy to establish the volume of material evaporated. The volume removed from the final, incompletely pierced layer was measured via optical microscopy and a depth probe. In this way the volume of the evaporated material was measured for each power/exposure time combination. Five holes were created for each combination given in Table 1. The results presented in figures 8 and 10 show the mean values and standard deviations of the results obtained.

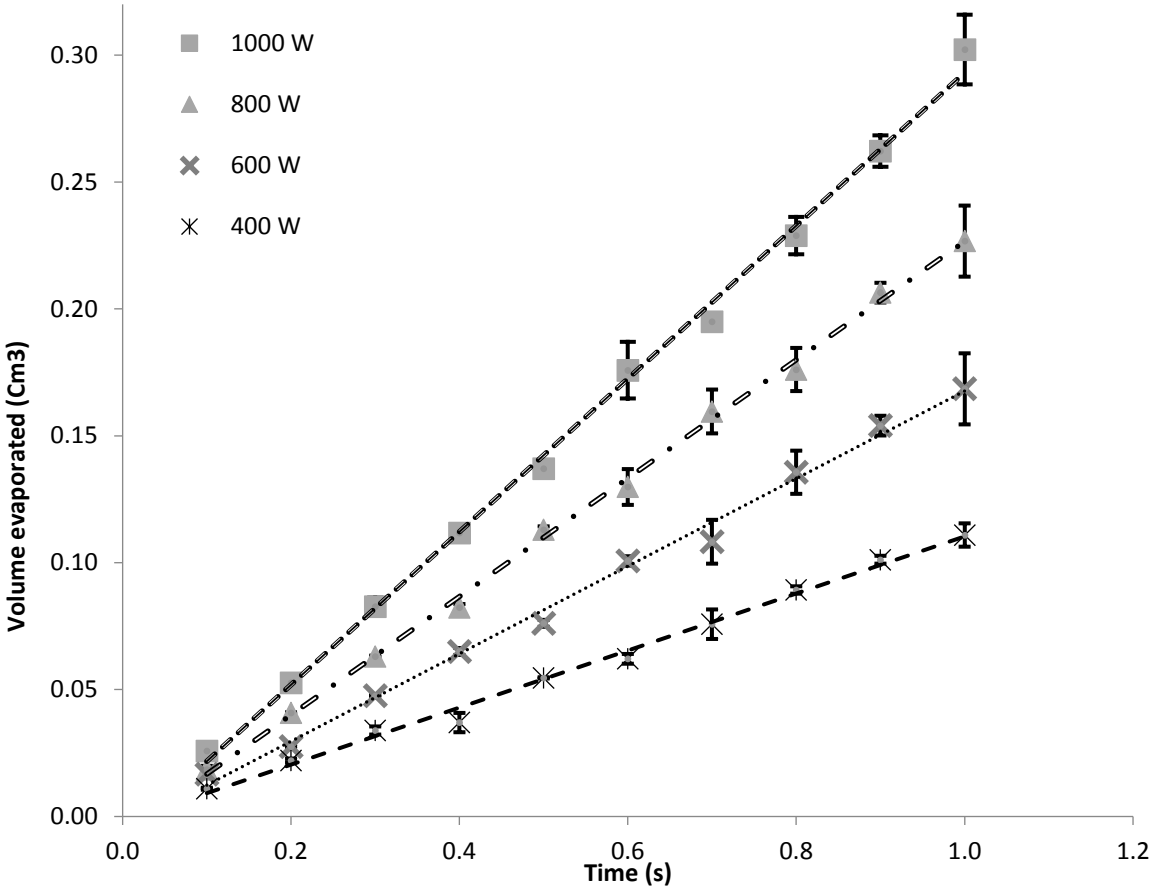

Figure 8. Evaporated hole volumes for different laser powers and exposure times, error bars indicate the standard deviation of measurements from five holes.

Figure 8 shows a linear relationship between hole volume and irradiation time for all power levels used. This suggests that the volume of material removed is proportional to the energy input.

Figure 9 is an optical micrograph of a typical cross section of the target material close to the surface after evaporation has taken place. It is apparent that the penetration depth of the 1µm light in this material has been limited to approximately 100 µm. In this 100 µm thick sub-surface layer there are pores which range in diameter from a few microns up to approximately 50 µm. The appearance of this layer is consistent with an evaporation process involving absorption of the laser light by carbon particles trapped in solid suspension within the otherwise transparent acrylic. The sub-surface layer represents a possible source of error in quantitative

analysis, since material has absorbed energy from the laser beam but has not been removed. This means that the relationship between energy input and volume of material removed is not entirely linear. However, our results show that this is a minor effect if the evaporated volume is considerably more than the residual melted layer.

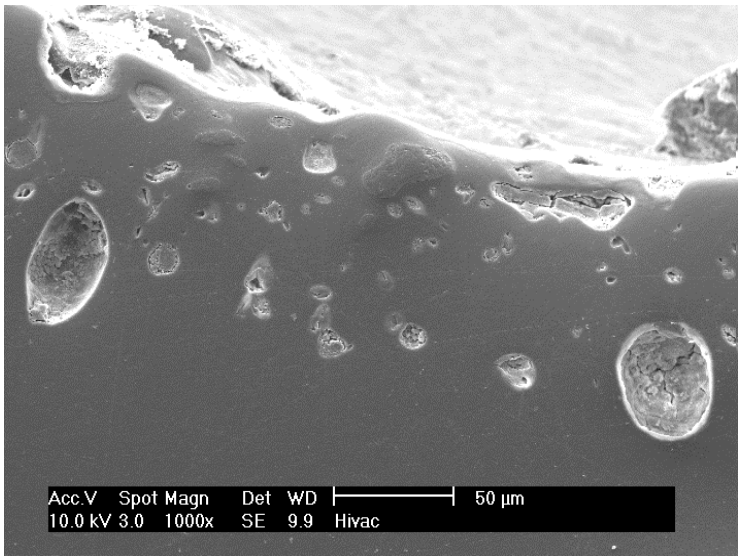

Figure 9 Micrograph of a cross section of the evaporated surface showing evidence of sub-surface boiling.

The results from figure 8 have been consolidated in figure 10 and it is clear that the results converge to give a very good straight line fit with a R^2 value of 0.9969.

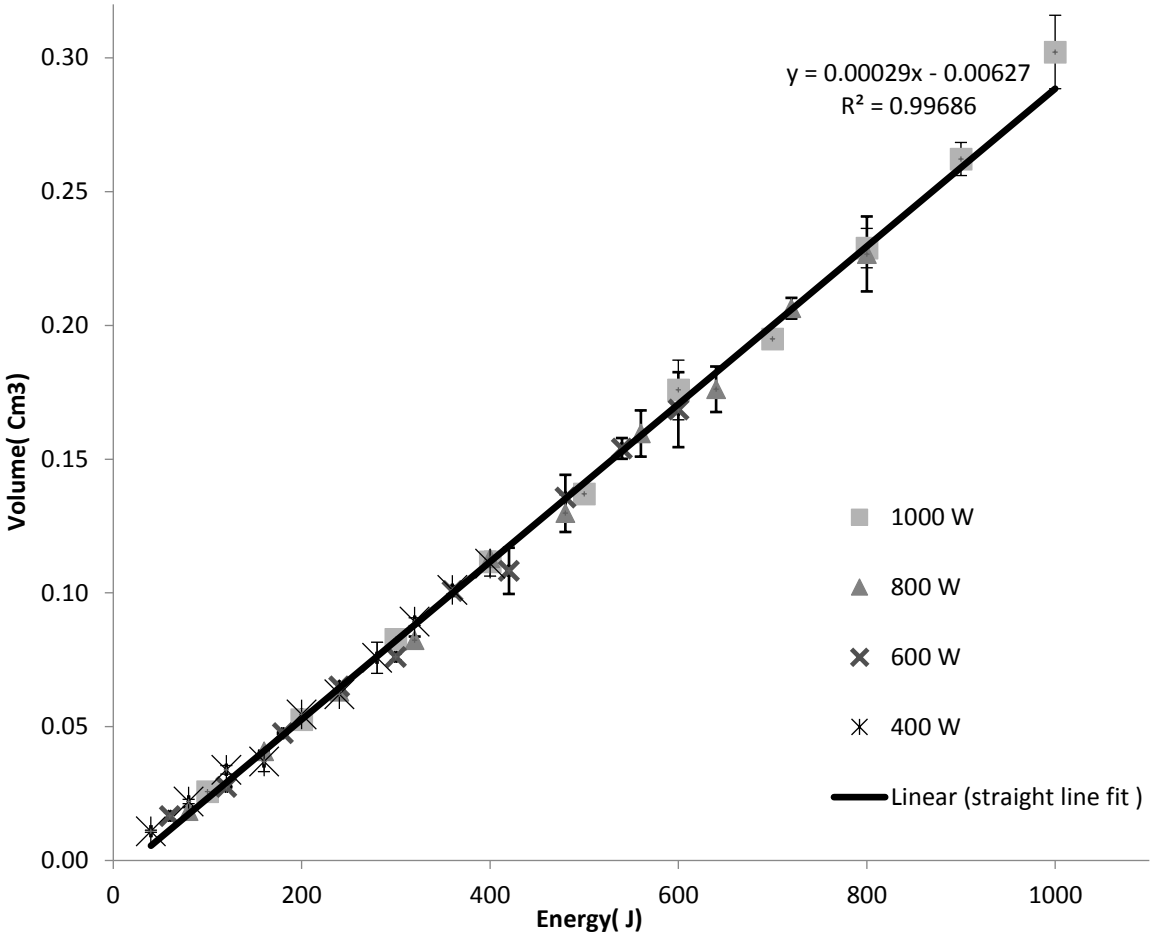

Figure 10. Volume of material evaporated as a function of energy.

From Figure 10 a specific evaporation energy of 3.44 kilojoules per cm^3 can be established, which is similar to, though slightly higher than, the 3.0 kJ cm^{-3} value found by Miyamoto et al.[4] for clear acrylic and CO_2 laser light. The 15% increase in specific evaporation energy can by attributed to the fact that the evaporation of carbon filled acrylic by a fibre laser is a two stage process, which is less efficient than the single stage process of transparent acrylic evaporation by CO_2 laser. The figure of 3.4kJ/cm^3 identified in this experiment is considerably smaller than the values obtained by Harris and Brandt [10] (4.5 – 5.5 kJ/cm3) and Scintilla et al. [9,14] (6.5 - 14.6 kJ/cm^3), and there are two main reasons for this. The first reason is explained in figure 11.

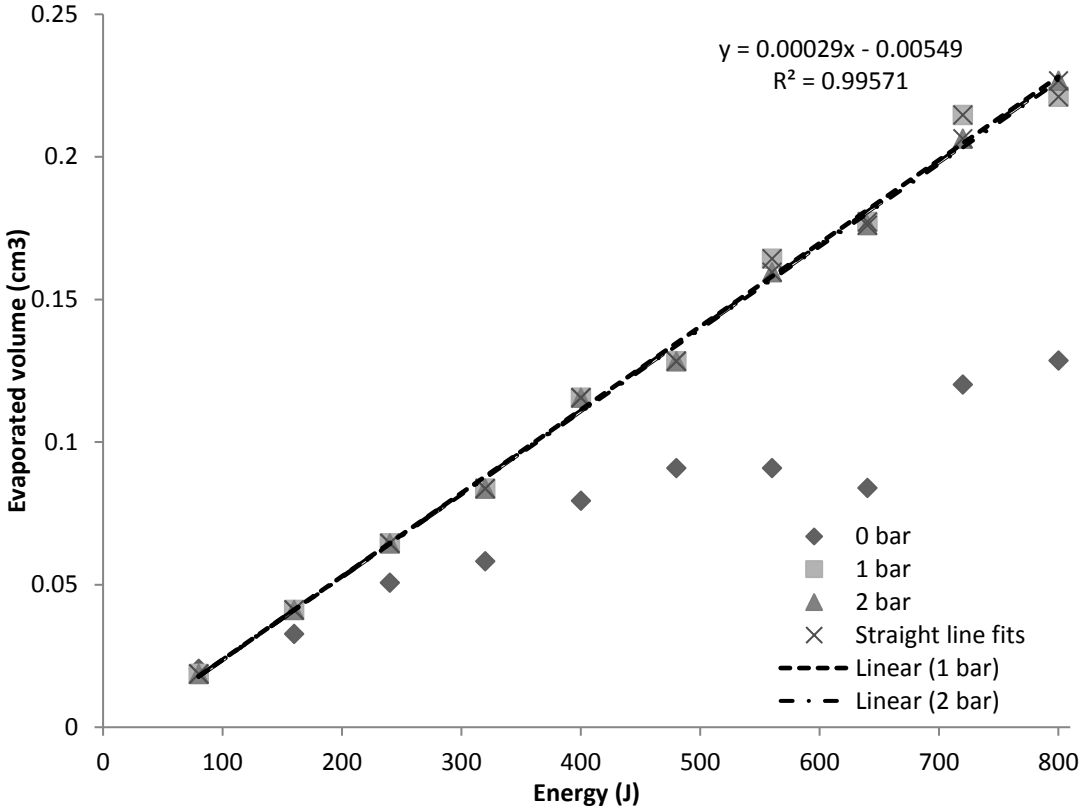

Fig. 11. Evaporated volume of carbon filled PMMA as a function of one micron wavelength laser energy for different flushing gas conditions (1mm diameter nozzle 6mm above the workpiece surface). A minimum gas flow is required to disperse the carbon dust/monomer plume above the evaporating surface.

Figure 11 demonstrates the effect of a flow of air or nitrogen in the laser-acrylic interaction zone. If such a jet is employed (and the beam is close to focus, and there is no movement between the laser and the acrylic), the evaporation volume is directly proportional to the incident energy as shown in figure 10. However, as mentioned earlier, the evaporation produces a plume of vapour which contains the monomer methyl methacrylate and carbon dust. This plume is extremely absorptive of the laser beam and, if it is not dispersed by a nitrogen or air jet, it will shield the underlying acrylic sample and dissipate the beam, resulting in fluctuating and artificially high figures for the specific energy of evaporation. In figure 11 the average

vaporisation energy rose to approximately 5.7 kJ/cm^3 and was non-linear in the absence of a flushing gas. Figure 11 shows that for the experimental set up used here, a 1 bar assist gas supply is sufficient to flush the vapour plume from the interaction area. One reason why the specific evaporation energy discovered here is considerably lower than those suggested by other workers is due to the effect of the flushing gas. The flushing gas used by Harris and Brandt [10] was not directed at the laser-acrylic interaction zone and was therefore probably only partially effective, and Scintilla et al. [9,14] did not use a flushing gas at all.

The second reason for the discrepancies between the specific heat of evaporation presented here and the results of earlier workers is related to threshold effects when the beam is moved relative to the acrylic target. Extrapolation of the straight line fit in figure 10 passes close to the origin, intersecting the x axis at a small positive value. This is consistent with a threshold which needs to be exceeded before degradation of acrylic, and subsequent material loss, occurs. This threshold effect can have a considerable effect on the amount of acrylic evaporated if the laser beam and the acrylic target are moving with respect to one and other (as was the case in the work carried out by Scintilla et al and Harris and Brandt). This subject will be discussed in more detail in the next section.

2.3 Problems associated with the measurement of primary losses during cutting.

Preliminary cutting experiments were carried out based on the type of experimental set-up described in figure 1 to determine how much laser energy leaves the bottom of the cut zone during fibre laser cutting of stainless steel. The work was carried out using a Bystronic 4kW fibre cutting machine which employs a moving head over stationary material (which is the standard set-up for modern flat-bed laser cutting machines). For these experiments therefore,

the cut material and the target acrylic sheet were both stationary and the laser head was moved at typical cutting speeds for the material involved (see table 2).

For each cut this resulted in an evaporated track in the acrylic sheet – as shown in figure 12a. A cross section of the groove (see figure 12b) could be measured later to estimate the volume of material evaporated per second during the cutting process. The cross-sectional area of the groove multiplied by the cutting speed multiplied by the specific energy of evaporation then gives a result related to the magnitude of the primary losses.

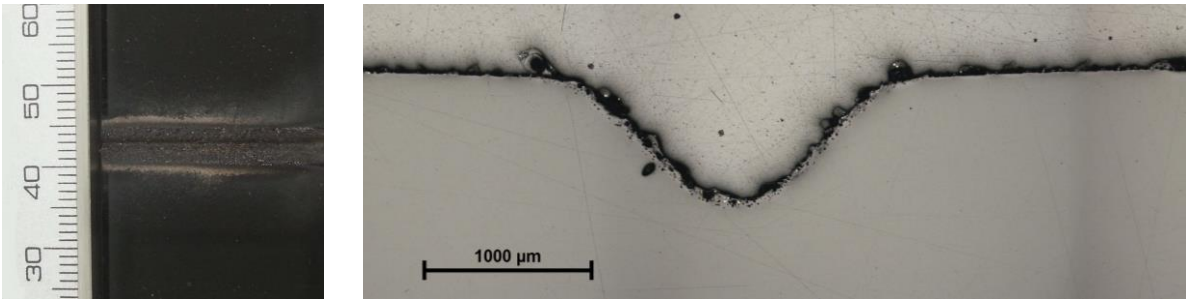

Figure 12. a. A view of the track evaporated form the surface of a carbon filled acrylic target placed 3mm below a stainless sheet which was being cut. b. The cross section of the evaporated track. From the scale on the left side it becomes obvious that the track has a width of more than 6 mm, which is much wider than the evaporated groove on the right side (less than 2mm). The wider, flat part of the track illustrates the existence of multi-reflected and scattered beam fractions.

The evaporation of any solid material by a laser beam involves overcoming a threshold energy density. As figure 9 shows, this threshold can be reduced to a trivial component of the overall interaction when dealing with a high power beam close to its focus on the surface of a stationary target. However, a broad, defocussed beam moving rapidly over the surface of a target might leave little or no trace of evaporation because the interaction does not exceed the threshold energy density (the threshold for, and rate of, evaporation is a function of the power density

and the speed of travel). A likely result is that a combination of movement and defocussing will result in an evaporation pattern which involves only a fraction of the primary losses.

In order to minimise threshold effects during the cutting/evaporated track experiments the target sheets of acrylic were placed as close as practicable to the bottom of the cut zone without interfering with the ejection of melt and cutting assist gas from the bottom of the cut. Initial trials indicated that a distance of 3mm was suitable and this was used when cutting 3mm, 4mm and 6mm thick material. This proximity of the acrylic target to the bottom of the cut zone had the advantage that a separate plume-flushing air jet was unnecessary, because the cutting gas jet itself flushed the plume from the area.

The results of the experiment are shown in table 2.

Thickness (mm)	Cutting speed (V, mm/s)	Cross sectional area of evaporated track (A, mm^2)	Energy required per second to generate evaporated track (VxAx3.4kJ/cm3) (Watts)	Energy required per second to generate evaporated track (VxAx3.4kJ/cm3) (% of input power)
3	166.7	0.73	414	10.3
4	103.3	1.24	435	10.9
6	56.7	2.34	451	11.2

Table 2. The results of the cutting trials; primary loss measurements.

The results given in table 2 suggest that the primary losses from the cut zone account for only approximately 11% of the output power of the laser in each case. The CALCut model suggests that at most 40-45% of the beam power is absorbed on the cutting front and contributes to the cutting process. However, this does not necessarily mean that a primary loss level of at least

55-60% could be detected below the sheet. In fact, the effects listed at the beginning of section 2.1 and described in more detail in the following section have to be taken into account.

There are a number of reasons why the experimental values for primary losses and theoretical values calculated from absorption estimates are so different. One consideration is the direction of travel of the reflected beam. In the case of a CO_2 laser cutting front the reflective surface is relatively smooth and almost vertical. This means that the reflected portion of the beam travels almost vertically downwards (as shown in figure 1) to impinge on the acrylic target. However, a fibre laser cutting front is covered in bumps, as demonstrated in the CALCut simulation presented in figure 13. The geometry of these bumps directs a proportion of the reflected beam back down the kerf where it is subject to more absorption/reflection interactions. This means that not all of the reflected beam interacts with the acrylic target.

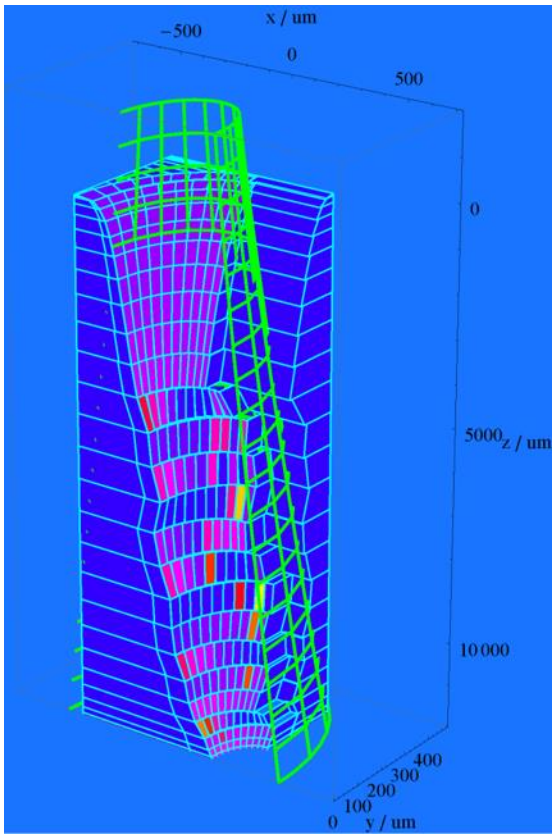

Figure 13. Cutting front calculated by CALCut including the distribution of the absorbed power density distribution during fibre laser cutting of 12 mm stainless steel [17].

Another consideration is the interaction of the beam with the stream of droplets leaving the cutting zone. The absorption events will remove energy from the beam and the scattering effect will reduce the energy density of some areas of the beam to below the threshold for evaporation of the acrylic.

In an attempt to identify the effect of beam movement and its associated threshold effects on these results, trials were carried out with a moving beam of known power moving across the surface of the target sheet. During these trials only the target acrylic was used and no metal cutting was involved. The beam was defocussed until tracks of similar width and cross sectional area were generated at the same cutting speed as the 3mm sample. It was discovered that an 800 Watt beam gave a similar groove shape (cross sectional area 0.76mm^3) at a process speed of 166.7mm/s (The same process speed as the 3mm sample cutting speed in table 2). Thus, at a laser-target relative speed of 166.7mm/s it takes 800 Watts to evaporate a groove who's volume indicates a power absorption of only 414 Watts (see table 2).

On top of this the divergence of the one micron wavelength beam leaving the bottom of the cut zone is very high compared to that of a CO_2 laser beam as a result of multiple reflections. Figure 14 indicates that multiple reflections tend to deflect the beam towards the horizontal and this results in a large divergence of the primary losses beam as it emerges from the bottom of the cutting zone.

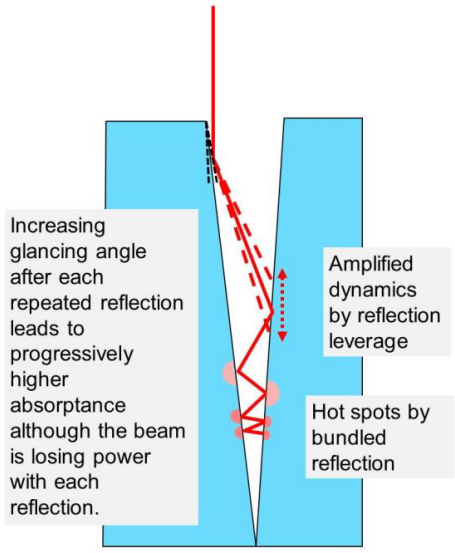

Figure 14. Multiple reflections tend to redirect rays from their original downward trajectory towards a more horizontal direction (ref 18).

The implication of these findings is that the results presented in table 2 are understated by a factor of two or more. Thus, it is clear that, although carbon black acrylic can give interesting qualitative information, and we now know the specific energy of vaporisation, threshold effects related to power density and travel speed need to be mapped, or calculated with reference to the specific energy of evaporation identified here, if the material is to be used for situations where the laser beam moves across the target.

Conclusions

It has been shown experimentally that carbon filled black acrylic can be employed as a quantitative tool for one micron wavelength fibre laser beams.

The laser power which is reflected off, and which passes through, the cutting zone during fibre laser cutting of stainless steel has a leaf type geometry of power density distribution indicative of a complex reflection history within the cutting zone.

The specific evaporation energy of carbon filled black acrylic is 3.4 kJ/cm^3.

Quantitative evaporation experiments will only yield a value of 3.4 kJ/cm^3 under the following conditions;

- The beam and the acrylic target must be stationary with respect to one and other.
- The beam must have sufficient intensity (high power, close to focus).
- There must be an air jet acting on the target zone sufficient to purge the area of the carbon-laden smoke.
- The volume evaporated must be much larger than the melted layer which remains on the sample surface.

If evaporation tests are to be carried out when the beam is moving relative to the target a compensation model based on 3.4 kJ/cm^3 needs to be used which takes into account the power density of the beam on the target surface and the speed of movement.

The total primary losses of the cutting process (i.e. laser output minus beam absorbed) cannot be accurately quantified by the evaporation of carbon filled acrylic because the primary loss 'beam' is subject to reflection and scattering processes which redirect and diffuse the beam out of the detection zone and/or to levels below the detection threshold.

References

1. J. Powell, A. Ivarson, L. Ohlsson, and C. Magnusson, "Energy redistribution in laser cutting," Welding in the World. **31**, 160-170 (1993).
2. C.L. Caristan, "Laser Cutting Guide for Manufacturing" Society of Manufacturing Engineers (2004).
3. J. Powell, "CO_2 laser cutting" Springer Verlag (1993).
4. L. Sarchin, "CO_2 Burn Samples - are they accurate?," Lasers and Optronics. 35-37 (July 1987).

5. I. Miyamoto, H. Maruo, and Y. Arata, "Intensity profile measurement of focused CO_2 laser beam using PMMA," in *ICALEO'84*, J. Mazumder, Editor. 1984, Laser Institute of America: Boston, MA, USA. p. 313-320.

6. J. Powell, A. Ivarson, and C. Magnusson, "An energy balance for inert gas laser cutting," Proceedings of SPIE - ICALEO'93, **2306**, 12-19 (1993)..

7. P. Di Pietro, Y.L. Yao, and A. Jeromin, "Quality optimisation for laser machining under transient conditions," Journal of Materials Processing Technology **97**, 158-167 (2000).

8. S.L. Ng, K.C.P. Lum, and I. Black, "CO2 laser cutting of MDF: 2. Estimation of power distribution," Optics & Laser Technology **32**, 77-87 (2000).

9. L.D. Scintilla, L. Tricarico, A. Wetzig, and E. Beyer, "Investigation on disk and CO2 laser beam fusion cutting differences based on power balance equation," International Journal of Machine Tools and Manufacture **69**, 30-37 (2013).

10. J. Harris, M. Brandt, and J. Powell, "Using black, opaque acrylic to analyse Nd:YAG laser beams," The Industrial Laser User. Association of Industrial Laser Users, **32**, 25 (2003).

11. R.I. Acosta, K.C. Gross, and G.P. Perram, "Thermal degradation of Poly(methyl methacrylate) with a 1.064 μm Nd:YAG laser in a buoyant flow," Polymer Degradation and Stability **121**, 78-89 (2015).

12. W.R. Zeng, S.F. Li, and W.K. Chow, "Review on chemical reactions of burning Poly(methyl methacrylate) PMMA," Journal of Fire Sciences **20**, 401-433 (2002).

13. J.G. Harris, and M. Brandt, "Visualisation of Nd:YAG laser beams using black PMMA," in Profiles in Industrial Research: Knowledge and Innovation 2002: St. Kilda, Victoria, Australia. 162-170 (2002).

14. L.D. Scintilla, L. Tricarico, A. Wetzig, A. Mahrle, and E. Beyer, "Primary losses in disk and CO2 laser beam inert gas fusion cutting," Journal of Materials Processing Technology **211** 2050-2061 (2011).

15. D. Petring, "Computer simulation of laser cutting for the limiting-value-oriented development of robust processes," Welding and Cutting **4** 37-42 (2005)

16. D. Petring, "Virtual Laser Cutting Simulation for Real Parameter Optimization," In Proceedings of the 84th Laser Materials Processing Conference, 84th JLPS meeting,. 11-18 (2016).

17. D. Petring, Cutting front calculated by CALCut. (2017). www.calcut.de/output/ (accessed June 26 2017).

18 D. Petring, T. Molitor, F. Schneider and N. Wolf." Diagnostics, modelling and simulation: three keys towards mastering the cutting process with fibre, disk and diode lasers,". Physics Procedia, 39, 186-196 (2012).